Oncogene (2016) **35,** 206–217

www.nature.com/onc

ORIGINAL ARTICLE

# DUSP10 regulates intestinal epithelial cell growth and colorectal tumorigenesis

CW Png[1,2], M Weerasooriya[1,2], J Guo[3], SJ James[1,2], HM Poh[1,2], M Osato[3], RA Flavell[4], C Dong[5], H Yang[3] and Y Zhang[1,2]

Dual specificity phosphatase 10 (DUSP10), also known as MAP kinase phosphatase 5 (MKP5), negatively regulates the activation of MAP kinases. Genetic polymorphisms and aberrant expression of this gene are associated with colorectal cancer (CRC) in humans. However, the role of DUSP10 in intestinal epithelial tumorigenesis is not clear. Here, we showed that DUSP10 knockout (KO) mice had increased intestinal epithelial cell (IEC) proliferation and migration and developed less severe colitis than wild-type (WT) mice in response to dextran sodium sulphate (DSS) treatment, which is associated with increased ERK1/2 activation and Krüppel-like factor 5 (KLF5) expression in IEC. In line with increased IEC proliferation, DUSP10 KO mice developed more colon tumours with increased severity compared with WT mice in response to administration of DSS and azoxymethane (AOM). Furthermore, survival analysis of CRC patients demonstrated that high DUSP10 expression in tumours was associated with significant improvement in survival probability. Overexpression of DUSP10 in Caco-2 and RCM-1 cells inhibited cell proliferation. Our study showed that DUSP10 negatively regulates IEC growth and acts as a suppressor for CRC. Therefore, it could be targeted for the development of therapies for colitis and CRC.

*Oncogene* (2016) **35,** 206–217; doi:10.1038/onc.2015.74; published online 16 March 2015

## INTRODUCTION

In the gastrointestinal tract, the mucus layer and the underlying intestinal epithelial cell (IEC) layer form a line of physical defence against luminal contents such as toxins and bacteria. Loss of this barrier function is characteristic of inflammatory conditions such as inflammatory bowel diseases.[1] Normally when the mucus layer is breached resulting in epithelial injury, epithelial-derived chemokines/cytokines are secreted resulting in the recruitment of immune cells.[2] At the same time, reconstitution of the damaged IEC will be initiated. Such 'wound healing' requires effective IEC proliferation and migration, which are on-going events in the intestinal epithelium for the maintenance of gut barrier function.[3]

Healing of the IEC layer involves multiple signalling pathways,[4–6] among which, ERK1/2 activation in IEC was shown to positively influence wound healing by driving IEC proliferation and migration.[6,7] Early activation of ERK1/2 is critical to healing in a rat model of gastric ulcers.[8] Additionally, *in vitro* wound healing assays showed rapid activation of ERK1/2 after 'wounding' in a monolayer of IEC.[6] Although ERK1/2 activation is critical for IEC proliferation to maintain gut homoeostasis, excessive or prolonged activation is deleterious and can result in tumorigenesis.[9] Increased ERK1/2 activation was shown to be a key downstream effector of the highly represented EGFR-KRAS-BRAF-MEK/ERK1/2 pathway in colorectal cancer (CRC).[10] Multiple gene mutations within this pathway that result in increased ERK1/2 activity is characteristic of CRC, as are alterations in other genes such as APC and p53.[11] Additionally, defective intestinal IEC barrier and chronic gut inflammation can further induce tumour development. In fact, inflammatory bowel diseases is one of the top three risk factors for CRC.[12,13]

Therefore, to ensure normal gastrointestinal function, mechanisms are in place to provide control of MAPKs activation (in this paper, 'MAPKs' refer to the three main MAPKs, namely ERK1/2, p38 and JNK1/2). One such measure is provided by dual specific phosphatases (DUSPs or MAPK phosphatases (MKPs)).[14] DUSPs and their activity in dephosphorylation of ERK1/2, p38 and JNK are well documented for their regulatory function in multiple tissues.[15,16] However, only few have examined the role of DUSPs in intestinal inflammation.[17] Most of these studies examined DUSPs in the context of immune cell regulation. Assessment of DUSPs in the IEC barrier function has not been clearly addressed.

In this study, we first examined the role of DUSP10 in intestinal inflammation. Wild-type (WT) and DUSP10 knockout (KO) mice were treated with dextran sodium sulphate (DSS) for the development of acute intestinal inflammation. Lower inflammation was observed in the KO mice, with increased IEC layer integrity and IEC proliferation. ERK1/2 activation and the expression of the cell proliferation-associated transcription factor, Krüppel-like factor 5 (KLF5), were increased in the KO colon. In line with increased IEC proliferation, DUSP10 KO mice developed more tumours upon DSS/azoxymethane (AOM) treatment than WT mice. Collectively, this study identified DUSP10 as an important regulator of intestinal epithelial barrier function and a suppressor of colon tumorigenesis.

[1]Department of Microbiology, Yong Loo Lin School of Medicine, National University of Singapore, Singapore, Singapore; [2]Immunology Programme, Life Science Institute, National University of Singapore, Singapore, Singapore; [3]Cancer Science Institute of Singapore, National University of Singapore, Singapore, Singapore; [4]Department of Immunology, Howard Hughes Medical Institute, Yale University, New Haven, CT, USA and [5]Department of Basic Medical Sciences, Tsinghua University School of Medicine, Beijing, China. Correspondence: Dr Y Zhang, Department of Microbiology, National University of Singapore, Centre for Life Science Institute, Immunology Programme, 28 Medical Drive, Singapore 117597, Singapore.
E-mail: miczy@nus.edu.sg
Received 30 August 2014; revised 4 January 2015; accepted 5 February 2015; published online 16 March 2015

## RESULTS

### DUSP10 KO mice were less susceptible to DSS-induced colitis with more intact IEC barrier

DSS treatment in WT mice resulted in reduced *Dusp10* expression in the colon (Supplementary Figure S1). DSS treatment damages the intestine epithelium resulting in exposure of the gut immune system to luminal contents. However, it is unclear whether the reduction of DUSP10 is acting as a feedback to allow increase MAPKs activation for induction of immune responses or an intrinsic protective mechanism to help the epithelium recover. Hence, to further examine the role of DUSP10 in gut inflammation, WT and DUSP10 KO mice were given 2% DSS for 5 days followed by 10 days recovery. Weight loss during DSS administration was comparable between WT and KO mice (Figure 1a). Weight recovery was observed in KO mice on Day 9, whereas, WT mice continued to lose weight and recovered on Day 13. After 5 days of DSS treatment, WT mice had shorter colon compared with KO (Supplementary Figure S2). Colonic histology showed less inflammation in KO mice where there were less cellular infiltrates, ulcers and epithelial erosions (Figures 1b and c). Colonic crypt architecture in KO mice was better preserved with more goblet cells after 5 days of DSS treatment. As such, it was not surprising that the DUSP10 KO mice continued to perform better during recovery. In line with the morphological findings, mRNA level of pro-inflammatory cytokine/chemokine genes was lower in KO colon (Figure 1d).

The results above suggested the presence of a protective mechanism limiting the amount of gut inflammation after DSS treatment in the KO mice. IEC layer acts as a barrier between the luminal contents and the mucosal immune system, which is critical for intestinal homeostasis. To assess IEC barrier integrity, the amount of fluorescein isothiocyanate (FITC)-dextran that

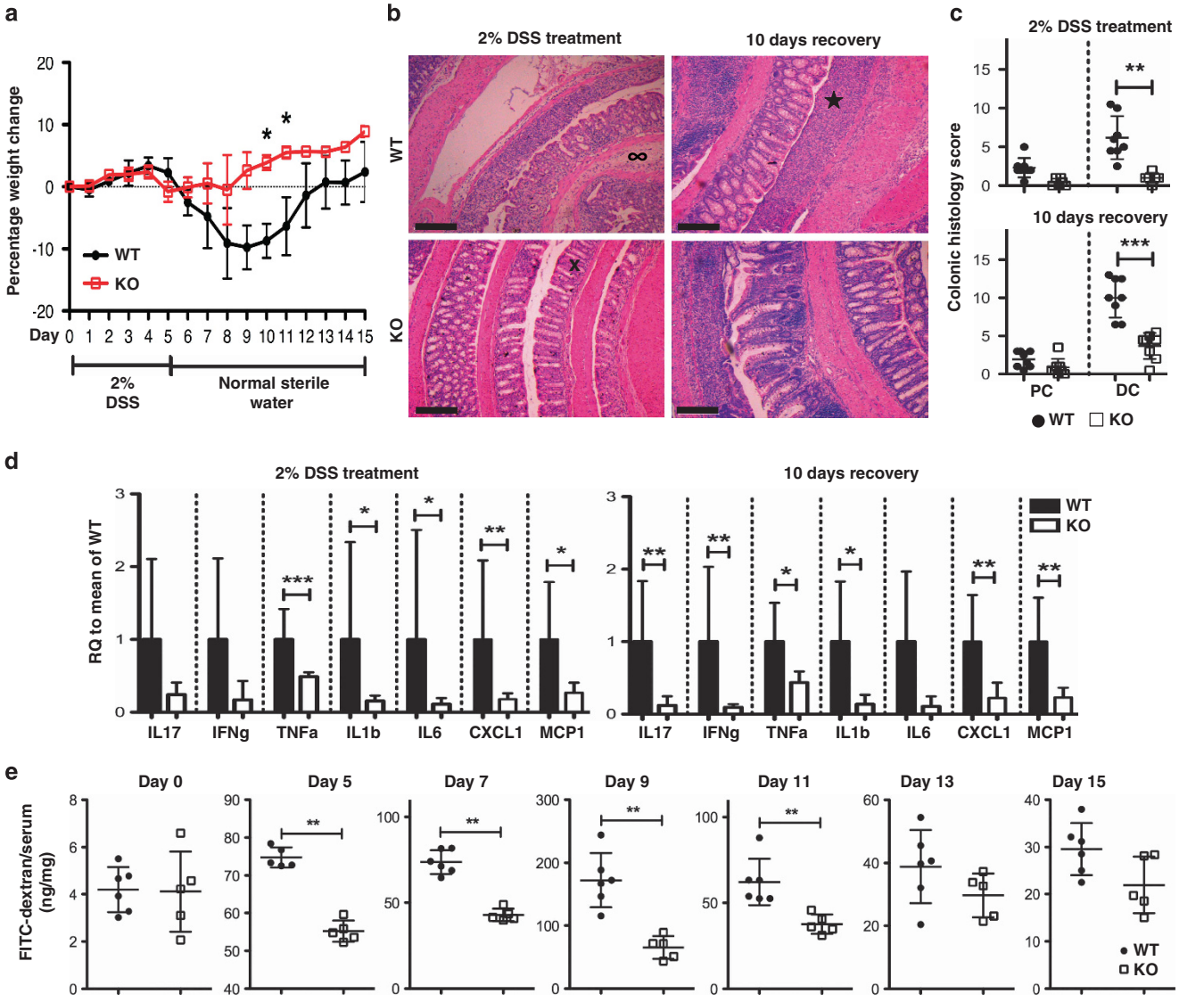


**Figure 1.** DUSP10 KO mice are resistant to DSS-induced colitis. (**a**) Percentage of weight change in mice during DSS treatment and recovery. (**b**) Representative histological micrographs showing colonic H&E stain. '∞', '★' and 'x' highlighted area with increased submucosal oedema, increased epithelial erosion/ulcers and better preserved crypt architecture with more goblet cells, respectively. Scale bar = 200 μm. (**c**) Scattered graphs showing colonic histological scores. PC and DC denote proximal and distal colon, respectively. (**d**) Colonic gene expression level relative to mean of WT. (**a**–**d**) Representative of 6–8 mice per group. (**e**) Level of intestinal permeability to FITC-dextran at day 0, at the end of DSS treatment (Day 5) and at various time points during 10 days of recovery. The data shown are a representative of 2–3 experiments. Data are presented as mean ± s.d. $^{*}P < 0.05$, $^{**}P < 0.01$.

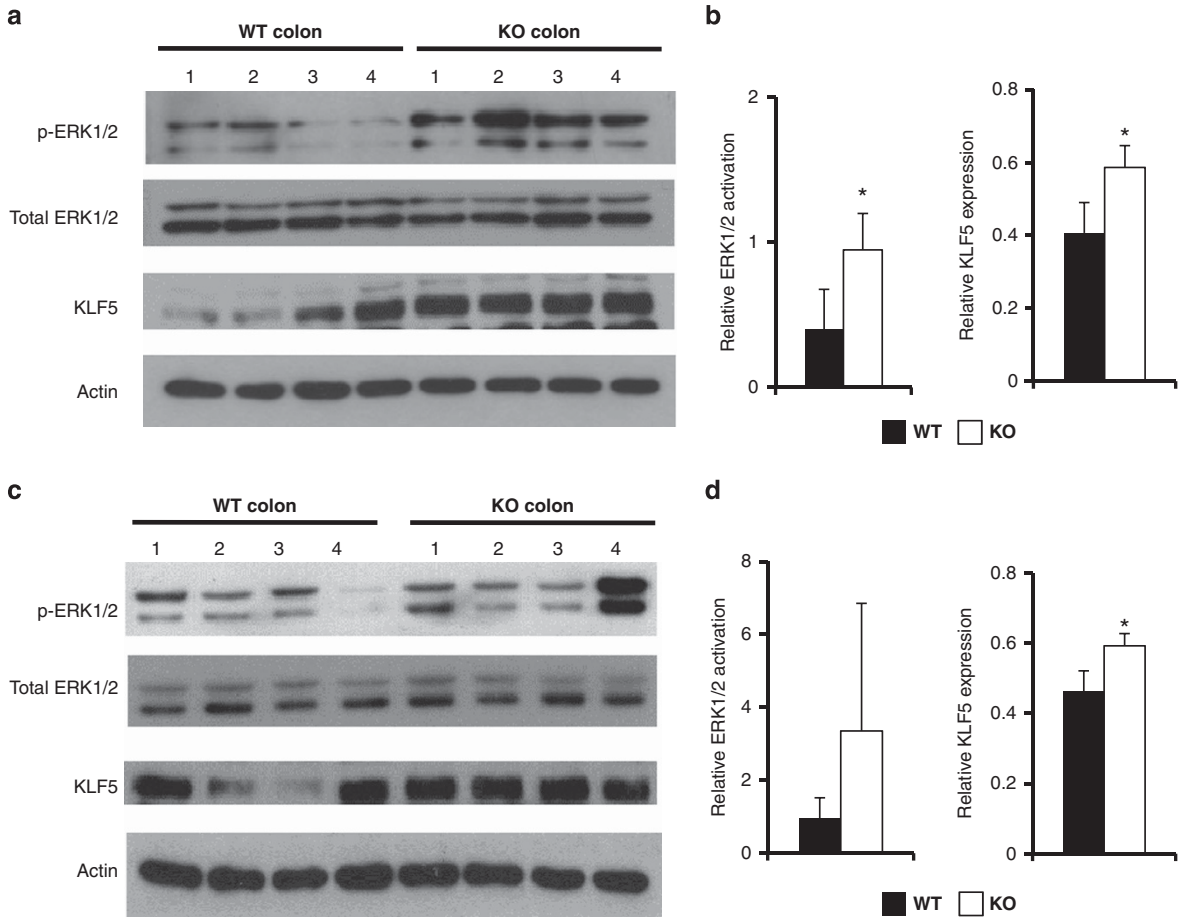


**Figure 2.** Increased ERK1/2 activation and KLF5 expression in DUSP10 KO colon. (**a**, **b**) Representative western blot and densitometric evaluation for ERK1/2 activation and KLF5 level in mice treated with 2% DSS for 5 days and (**c**, **d**) 2% DSS for 5 days with 10 days recovery. Results shown are representative of 6–8 mice per group. Error bars = s.d. $^*P < 0.05$.

'leaked' through the epithelium was measured in response to DSS treatment. Serum FITC-dextran was increased after DSS treatment in all mice (Figure 1e), however, it remained lower in DUSP10 KO mice compared with WT at all time points. On Day 5, the amount of serum FITC-dextran was 1.3-fold lower ($P = 0.008$) in KO mice. For both strains, the amount of serum FITC-dextran peaked at Day 9, but it was 2.6-fold lower ($P = 0.004$) in KO mice. To note, there was less fluctuation of serum FITC-dextran levels in KO mice from Day 5, 7–9, where mean serum FITC-dextran was 54 ± 13.0038 ng/ml. On the other hand, the mean serum FITC-dextran level across the three time points in WT was 109 ± 54.2 ng/ml. This clearly showed that the intestinal epithelial barrier was more intact in DUSP10 KO mice after DSS administration.

### Increased ERK1/2 activation and KLF5 expression in DUSP10 KO colon after DSS treatment

Further analysis of the changes in MAPKs activation in the colon showed that ERK1/2 activation was increased in KO mice compared with WT mice after 5 days of DSS treatment (Figures 2a and b, Supplementary Figure S3). However, the amount of colonic p-ERK1/2 was not significantly different between WT and KO after 10 days recovery ($P = 0.114$) (Figures 2c and d). On the other hand, p38 and JNK1/2 activation was comparable (Supplementary Figure S4). Interestingly, the expression of KLF5, an ERK1/2 associated transcription factor and a key player in epithelial regeneration,[18] was significantly increased in KO colon after DSS treatment and at the end of recovery (Figure 2). We further found that the expression of cyclin B1, a KLF5 target gene that is critical for cell proliferation,[19] was increased by 1.9-fold after recovery in KO compared with WT colon (Supplementary Figure S5). It is known that p-ERK1/2 is a key activator in the IEC wound healing response.[6] In the gut, KLF5 is mainly expressed by IEC.[20] It is important for the maintenance of intestinal crypt architecture and is a positive regulator for wound healing and cell proliferation after DSS treatment.[21,22] Together, these data suggested that deficiency of DUSP10 resulted in increased ERK1/2-KLF activation/expression in the gut, which could provide better wound healing and maintenance of the IEC barrier.

### DUSP10 overexpression in IEC suppresses ERK1/2 activation, KLF5 expression, wound healing and cell proliferation

To further confirm that DUSP10 regulates ERK1/2-KLF5 in epithelial cells, CMT93 (mouse intestinal epithelial cell line derived from induced carcinoma of mouse colon) stably overexpressing DUSP10 (Supplementary Figure S6) was generated. CMT93-dusp10 (overexpressing DUSP10) and CMT93-pcdna cells (vector control) were treated with 5% DSS to assess ERK1/2 activation. We observed that ERK1/2 activation peaked at 10 min post DSS treatment in both CMT93-dusp10 and CMT93-pcdna cells (Figure 3a). However, the level of p-ERK1/2 in CMT93-dusp10 cells was lower at all time points. The regulation of ERK1/2 activation by DUSP10 was further supported by the *in vitro* assessment of phosphatase activity of DUSP10 on ERK1/2. Supplementary Figure S7 shows that DUSP10 is capable of dephosphorylating ERK1/2.

Consistent with increased KLF5 expression in DUSP10 KO colon, overexpression of DUSP10 in CMT93 cells greatly reduced KLF5

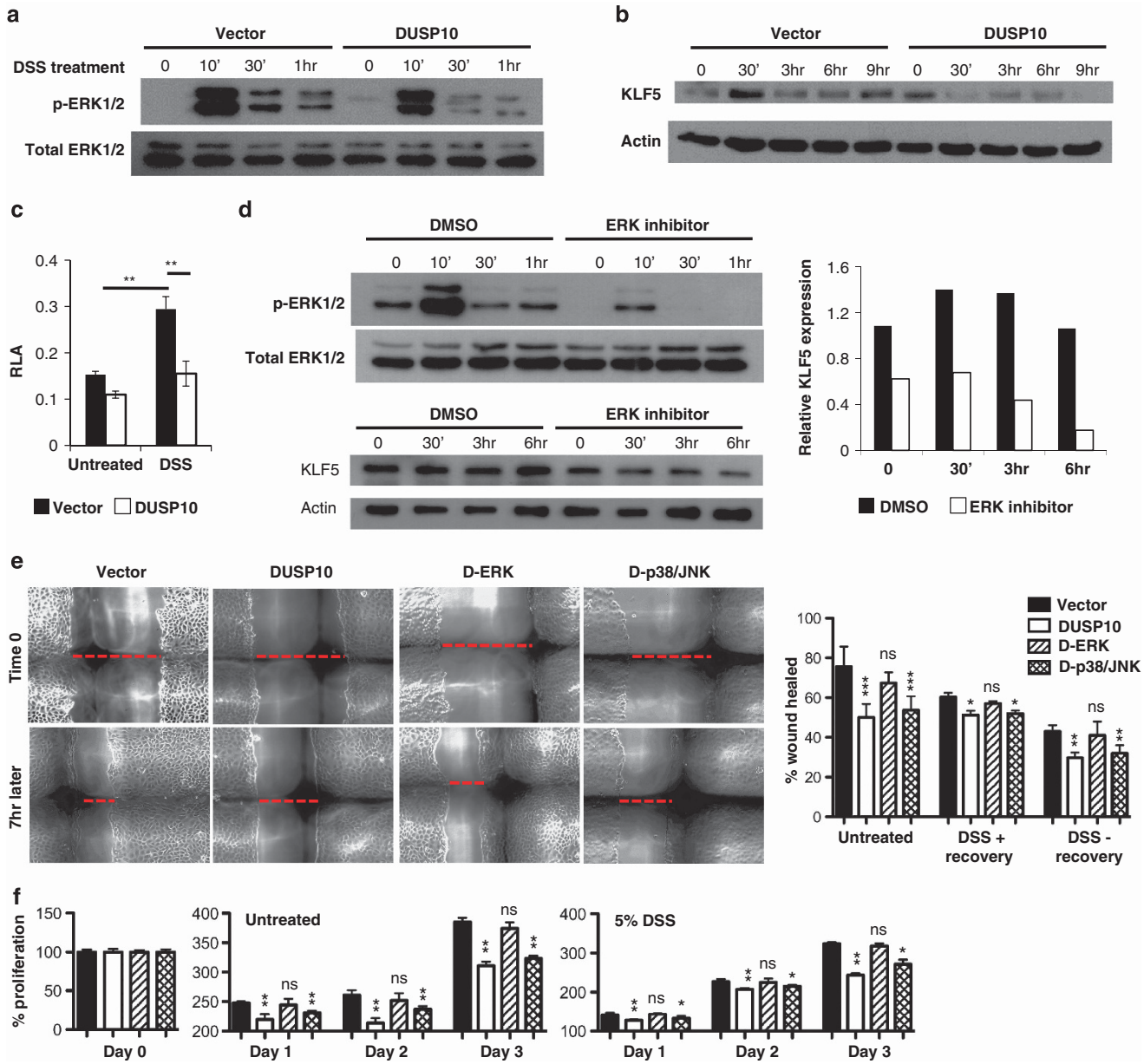


**Figure 3.** Overexpression of *Dusp10* in CMT93 inhibits ERK1/2-KLF signalling, proliferation and wound healing. (**a**, **b**) ERK1/2 activation and KLF5 expression in response to 5% DSS treatment in CMT93-dusp10 and CMT93-pcdna (Vector) cells were determined by western blot analysis. (**c**) Dual luciferase assay was used to examine the effect of *Dusp10* overexpression on *Klf5* promotor activity. The KLF5 promoter activity was normalised to the internal control renilla activity (RLA: relative luciferase activity). (**d**) Representative western blot showing effect of ERK inhibition on KLF5 expression in CMT93 cells treated with 0.2% DSS. Bar chart shows the ratio of KLF5 to actin level based on the densitometry analysis. (**e**) Representative micrographs showing *in vitro* wound healing of untreated CMT93-vector, CMT93-DUSP10, CMT93-DUSP10 lacking the ERK binding site (D-ERK) and CMT93-DUSP10 lacking the p38/JNK binding site (D-p38/JNK). Bar charts showing the percentage of wound recovery. All cells were pre-treated with 5% DSS for 24 h except cells in untreated group. Normal culture medium was used during the 7- h 'wound period' for cells with recovery as opposed to cells without recovery that were cultured in medium with 5% DSS. (**f**) Bar charts showing the percentage of cell growth with or without 5% DSS treatment. DUSP10, D-ERK and D-p38/JNK denote cells overexpressing full-length DUSP10, DUSP10 with deletion of the ERK binding site and DUSP10 with deletion of p38/JNK binding sites, respectively. Results shown are representative of four experiments. Error bars = s.d. $^{*}P < 0.05$, $^{**}P < 0.01$.

expression after DSS treatment (Figure 3b and Supplementary Figure S8). KLF5 promoter activity, which can be induced by DSS, was also significantly repressed by overexpression of DUSP10 in CMT93 cells (Figure 3c). Expression of KLF5 targets, epidermal growth factor receptor (EGFR) and cyclin-B1,[22] which regulates wound healing, was also reduced in CMT93-dusp10 cells (Supplementary Figure S8). Previous studies have shown that KLF5 can regulate EGFR and downstream ERK1/2 activity, which in turn regulate the level of KLF5.[21,23] Hence, the regulation of KLF5-EGFR-ERK-KLF5 form a feedback loop system and DUSP10 can be involved in controlling ERK1/2 activation in this loop system. Interestingly, the regulation of KLF5 by ERK1/2 may also be cell type dependent. Previous study by Mori *et al.*[24] showed that KLF5 was only regulated by ERK in IEC but not in pancreatic cells. Indeed, in line with others,[19,25] ERK1/2 inhibition dampened KLF5 expression in CMT93 epithelial cells (Figure 3d). Whereas JNK

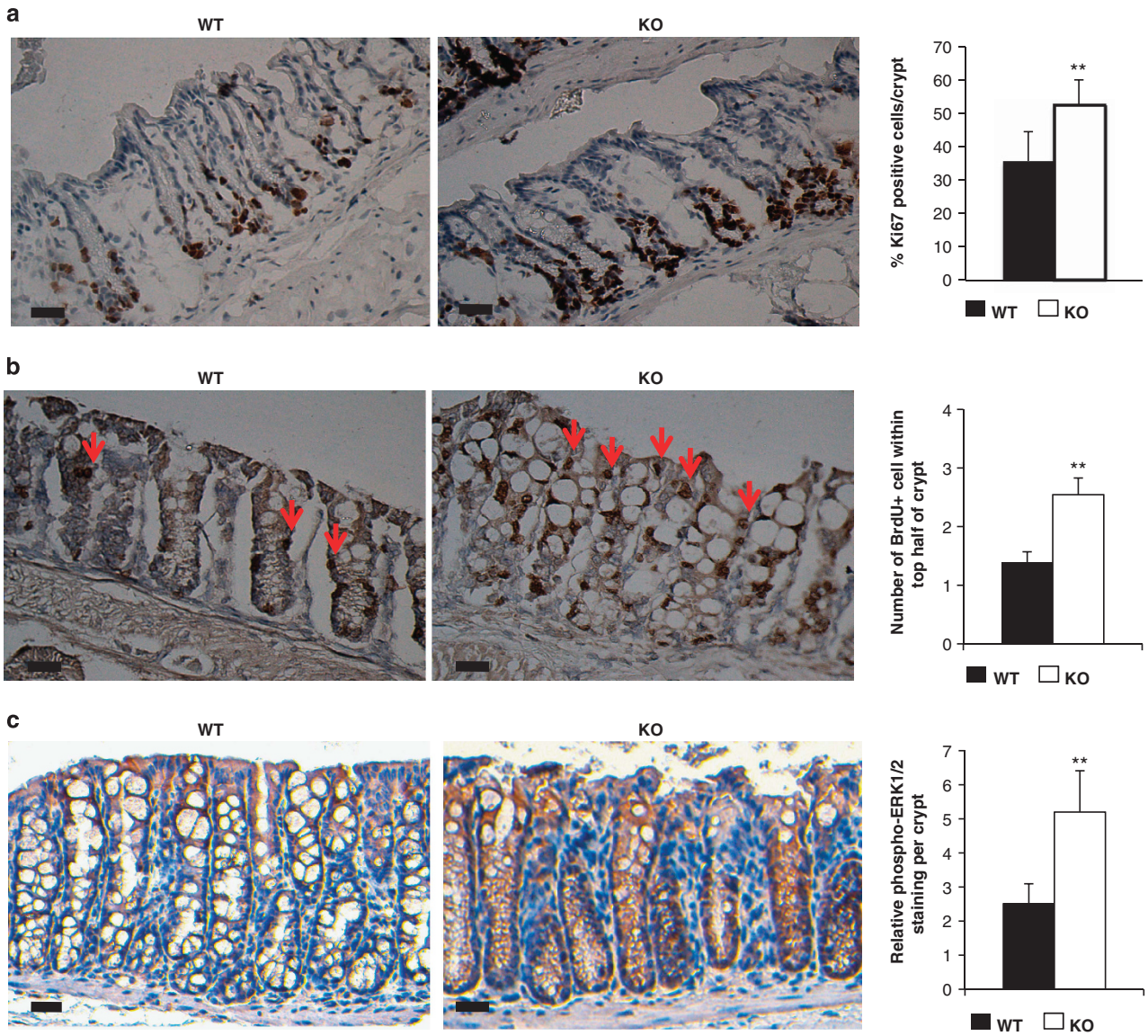


**Figure 4.** Increased epithelial cell proliferation in DUSP10 KO colon after DSS treatment. Assessment of colonic EC migration/proliferation *via* BrdU and Ki67 immunohistochemistry staining in mice given 2% DSS for 5 days. (**a**) Representative micrographs of colonic sections stained for Ki67 and bar chart showing the percentage of Ki67-positive cells per crypt. 15–18 full-length crypts were counted per mouse colon. (**b**) Representative micrographs of colonic sections stained for BrdU. Arrows highlight BrdU-positive cells nearest to the crypt surface. Bar chart showing the percentage of BrdU-positive cells found within the top half of each crypt. (**c**) Representative micrographs of colonic sections stained for phospho-ERK1/2. Bar chart shows the relative staining intensity of phospho-ERK1/2. Scale bar = 25 μm. Error bars = s.d. $^{**}P < 0.01$.

inhibition during DSS treatment did not significantly changes the expression of KLF5 and p38 activation was not observed after DSS treatment (Supplementary Figure S9). Taken together, it is evident that DUSP10 negatively regulate ERK1/2, which in turn reduced KLF5 expression in IEC.

Next, we examined the role of DUSP10 in regulating IEC wound healing. At basal level, overexpression of DUSP10 was sufficient to retard wound healing in CMT93-dusp10 monolayer compared with CMT93-vector (Figure 3e 'untreated'). To mimic DSS-induced damage, cells were pre-treated with 5% DSS for 24 h, after which a scratch was introduced. The cells were then left to heal in medium with or without DSS that mimic the conditions of without or with recovery, respectively. There was less wound healing in CMT93-dusp10 monolayer in all conditions. At the same time, we found that CMT93 overexpressing DUSP10 had reduced growth with or without 5% DSS (Figure 3f). To test whether DUSP10 interaction with ERK1/2 or p38/JNK is important for its regulation on cell growth, we generated DUSP10 mutants where the domain required for its interaction with ERK1/2 or p38/JNK was deleted as described previously.[26,27] Reduced wound healing and cell proliferation were also observed in CMT93 cells stably over-expressing DUSP10 lacking the binding site for p38 and JNK (Figures 3e and f). The level of reduction was similar to that of CMT93 overexpressing full-length DUSP10 ($P > 0.05$). On the other hand, deletion of ERK binding site showed no significant change in proliferation and wound healing compared with the vector control. Together, these results demonstrated that DUSP10/MKP5 inhibits wound healing through inhibiting ERK1/2 activation and

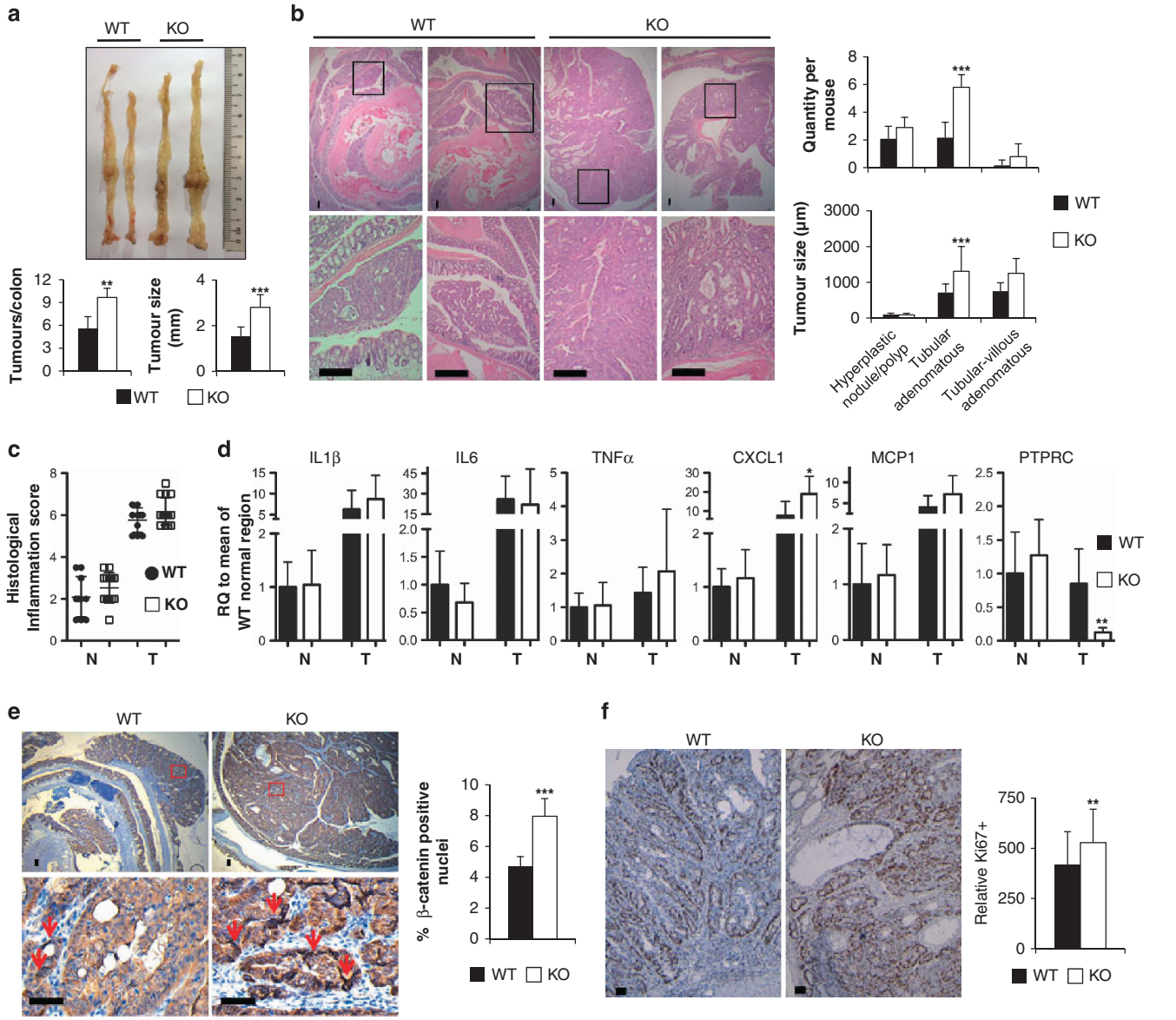


**Figure 5.** Increased colon tumour development in DUSP10 KO mice after AOM/DSS treatment. (**a**) Representative photograph showing the most severe and the mildest colonic tumour growth from each mouse group. Bottom bar charts showing the multiplicity and size of the tumours based on macroscopic assessment. (**b**) Representative micrographs showing H&E stain of colonic tumours. Boxed area was magnified and presented in the respective bottom panel. Bar charts showing the quantitative assessment of each type of polyp. (**c**) Scattered graph showing inflammatory scores for tumours and macroscopically normal region adjacent to the tumours. (**d**) Colonic inflammatory cytokine and chemokine gene expression level relative to mean of WT normal region. 'T' and 'N' denote tumours and macroscopically normal region next to the tumour, respectively. (**e**) Representative micrograph of β-catenin immunohistochemistry staining in tumour tissues. Boxed regions were magnified and present under the respective panels. Red arrows highlighted nuclear β-catenin stains. Percentage β-catenin staining per microscopic view of tumour is represented in the bar chart. (**f**) Representative micrograph of Ki67 immunohistochemistry staining and bar chart showing relative level of Ki67 stain in tumour tissues. Results shown are representative of 2 experiments each having 9–12 mice per group. Error bars = s.d. Scale bar = 50 μm. $^{*}P < 0.05$, $^{**}P < 0.01$, $^{***}P < 0.001$.

KLF5 expression, in accord with earlier work where reduced p-ERK1/2 or KLF5 expression resulted in worse wound healing *in vitro*.[6,28]

## Increased IEC proliferation and ERK1/2 activation in DUSP10 KO mice in response to epithelial damage

Results above show that DUSP10 can negatively regulate ERK1/2 activation and KLF5 expression to suppress epithelial wound healing. Conversely, in DUSP10 KO mice, the increased IEC healing could explain the reduced epithelial permeability, thus limiting gut inflammation in response to DSS. We therefore measured IEC proliferation, a key process in intestinal wound healing. The extent of IEC proliferation was determined by Ki67 immunohistochemistry staining. As shown in Figure 4a, there were increased numbers of Ki67-positive cells, with higher staining intensity, within the bottom and along the crypts of DSS-treated KO colon compared with WT. In addition, staining of incorporated 5-bromo-2-deoxyuridine (BrdU) showed more BrdU-positive cells were found along the length towards the top of the crypts in DUSP10 KO mice as opposed to WT mice where the BrdU-positive cells were mainly at the bottom half of the crypts (Figure 4b).

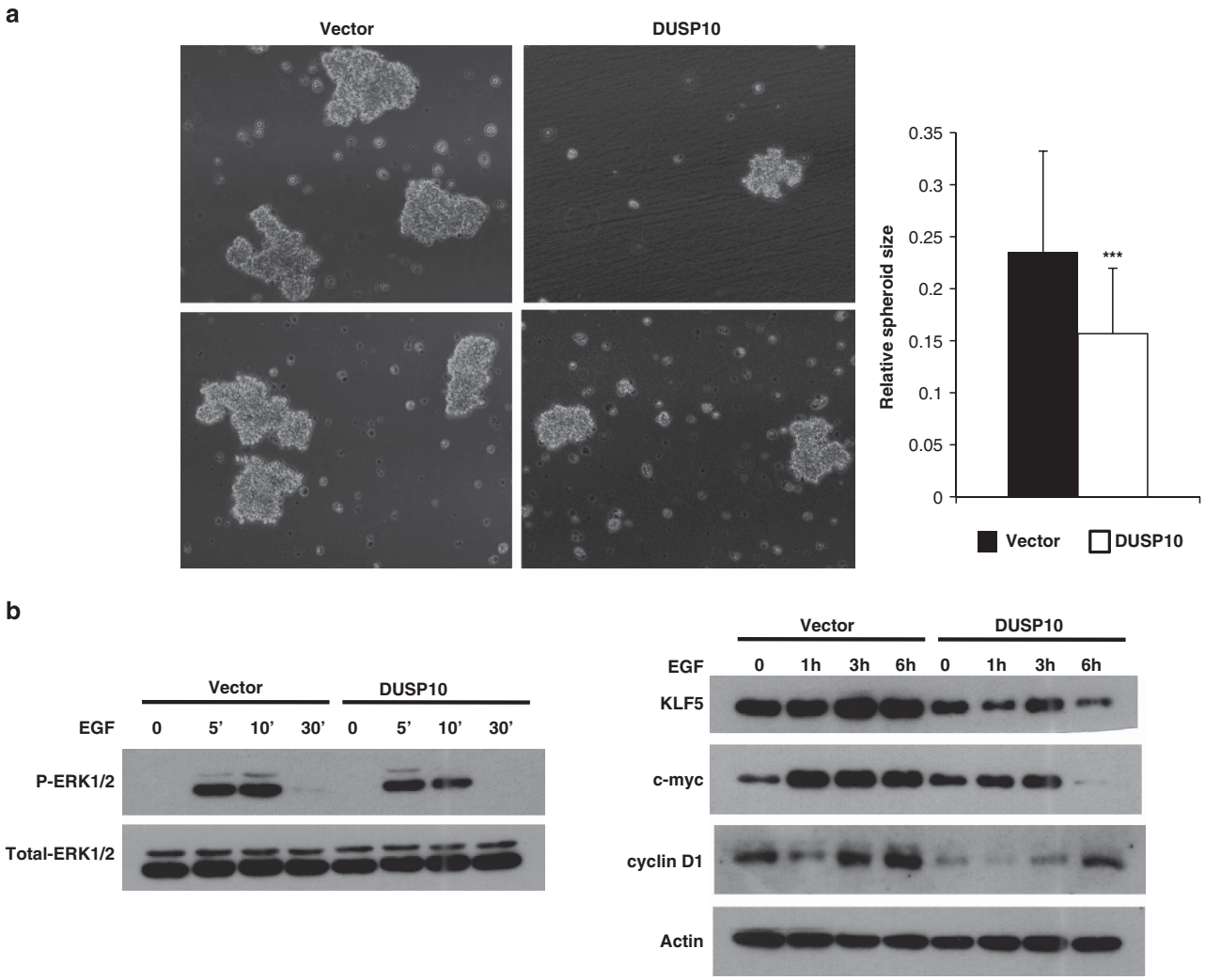


**Figure 6.** DUSP10 inhibited cellular spheroid formation and downregulated ERK1/2 targeted proteins associated in cell proliferation. (**a**) Representative micrographs of multicellular spheroid aggregates and bar chart showing the size of the spheroids derived from the respective CMT93 cells. Error bars = s.d. Scale bar = 50 μm. ***$P < 0.001$. (**b**) Representative western blot showing the effect of DUSP10 overexpression in CMT93 cells after EGF (50 ng/ml) stimulation. Results shown are representative of three independent experiments.

There were 1.8-fold more ($P = 0.004$) BrdU-positive cells within the top half of the intestinal crypt of KO mice. This in all suggest that the increased IEC proliferation in DUSP10 KO provided a pool of new epithelial cells to replace the damaged IEC so that the epithelium maintains its continuity. In addition, p-ERK1/2 staining was overall increased in the colon epithelial cells of KO mice after 5 days of DSS treatment (Figure 4c). This is in line with the increased level of p-ERK1/2 found by western blot analysis shown in Figure 2a.

### Colonic IEC proliferation in DUSP10 KO mice contributes to increased susceptibility to AOM/DSS-induced tumour development

Although increased IEC proliferation was protective in acute inflammation, excessive IEC proliferation may lead to colon tumour development. ERK1/2 is a key downstream activator of the EGFR-KRAS-BRAF-MEK pathway. On the other hand, KLF5 has also been implicated in intestinal tumorigenesis.[18,29] Therefore, increased ERK1/2 activation and KLF5 expression in DUSP10 KO colon might elevate the likelihood of tumour development. To examine whether DUSP10 has a role in intestinal tumorigenesis, colonic tumours were induced in mice using AOM and 1% DSS treatment. In this model, chronic administration of 1% DSS provided the stimulant for continuous increased IEC growth, whereas AOM allows the induction of DNA mutation within the colonic cells.[30] We found that DUSP10 KO had more colonic tumours with larger size (average size of 2.6 mm) compared with WT (tumour average size of 1.5 mm) within the mid- to distal-colon (Figure 5a and Supplementary Figure S10). Histologically, adenomatous polyps were more prominent in KO mice (Figure 5b). There were 2.6-fold more tubular adenomatous polyps in KO mice with an average size of 1.3 mm than in WT mice (average adenomatous polyps size: 0.7 mm). The level of inflammation was comparable between WT and KO tumours and normal region in the colon based on the histological assessment (Figure 5c). In addition, there was no significant difference in the level of pro-inflammatory cytokine and chemokine gene expression in normal region adjacent to the tumours (Figure 5d). *Cxcl1*, a monocyte chemokine was increased only in tumours of KO mice, whereas the pan-leukocyte marker PTPRC gene was reduced by 6.7-fold ($P = 0.005$) in the tumours of KO mice. Increased nuclear accumulation of β-catenin and Ki67 staining was also detected in KO tumour tissues (Figures 5e and f). Accumulation of nuclear β-catenin is often seen in CRC patients and is a sign of Wnt pathway activation, which induces the expression of cell cycle-related genes such as cyclin-D1 and c-Myc.[31] AOM treatment was

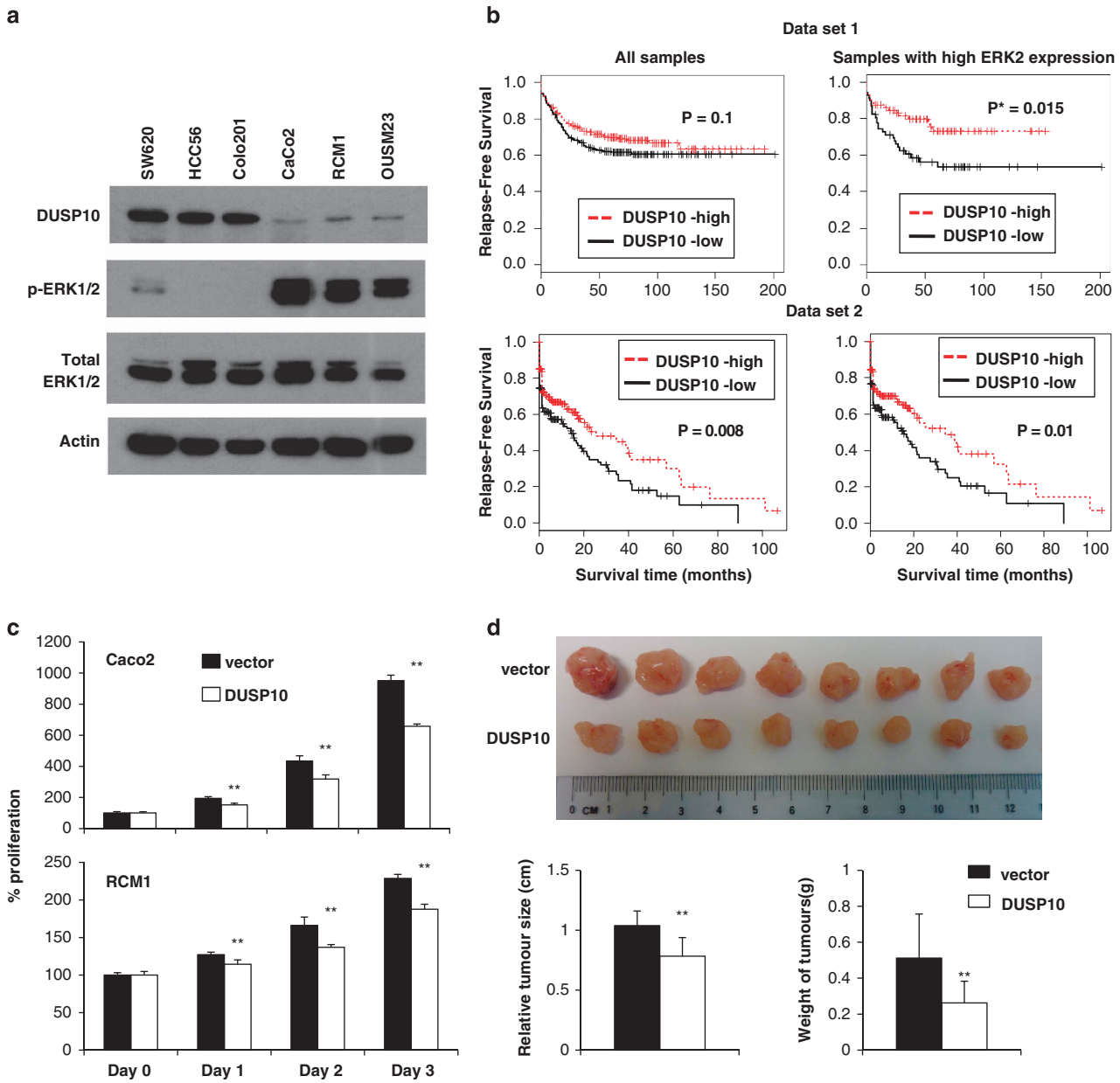


**Figure 7.** Increased DUSP10 expression is correlated with better survival in CRC patients. (**a**) Western blot showing the level of DUSP10 and p-ERK1/2 at basal state in human CRC cell lines. (**b**) Survival data analysis using data available from Data Set 1; Marisa *et al.*[34] and Data Set 2; The Cancer Genome Atlas[35] based on Kaplan–Meier method. In Data Set 1, left panel shows analysis of all 557 CRC patients' tumour samples. Right panel shows the analysis of 149 (out of total 557) CRC patients' samples with high ERK2 expression. In Data Set 2, left panel shows analysis of 404 CRC patients' tumour. Right panel shows the analysis of 291 (out of total 404) CRC patients samples with high ERK2 expression. (**c**) Decreased proliferation of Caco2 and RCM-1 cells overexpressing DUSP10. Bar chart shows the relative fold change in cell proliferation/growth. (**d**) Representative pictures of Caco2 xenograft tumours developed in NOD/SCID mice. Bar charts show the relative size and weight of the tumours harvested from the mice at end point. Error bars = s.d. $*P < 0.05$, $**P < 0.01$.

known to induce mutation in β-catenin gene leading to accumulation for colon carcinogenesis.[32,33] The excessive IEC proliferation in the KO mice could contribute to further overall increase in gene mutation rate leading to increased β-catenin nuclear accumulation.

Together with the increased Ki67-positive cells shown in colitis model (Figure 4a) and in tumour (Figure 5f), our data suggest that the epithelial cells and the subsequent tumours that were formed were more proliferative in the absence of DUSP10, and hence led to the increased tumour number and size found in the KO mice. Similarly, evidence from *in vitro* multicellular spheroid aggregate formation assay demonstrated that overexpression of DUSP10 retard the formation of spheroids. As shown in Figure 6a, CMT93 overexpressing *Dusp10* had reduced capacity to develop multicellular tumour spheroid aggregates than CMT93-vector cells. After 5-day culture, the CMT93-dusp10-derived spheroids were on average 1.5-fold smaller than those formed from CMT-vector cells. This could result from the reduced rate of cell proliferation in CMT-dusp10 (Figure 3f), from reduced aggregation ability of the cells to form a spheroid structure, or both. In addition, overexpression of DUSP10 resulted in reduced ERK1/2 activation upon EGF stimulation (Figure 6b, left panel). In turn, key downstream components, KLF5, c-myc and cyclin D1, involved in proliferation were also reduced (Figure 6b, right panel).

Increased *Dusp10* expression is associated with better survival rate in CRC patients

The strong pro-tumorigenic phenotype found in our model demonstrated that DUSP10 clearly has a functional role in the development of intestinal tumours *in vivo*. To understand whether DUSP10 may be involved in human CRC, we first assessed DUSP10 expression in human CRC cell lines. DUSP10 protein was expressed in all six CRC cell lines examined. Consistent with experimental studies above, the protein level of DUSP10 was inversely related to the level of p-ERK in these cell lines (Figure 7a and Supplementary Figure S11). To further investigate the clinical relevance of DUSP10 expression in colorectal tumours, detailed analysis of a recently published survival data set from Marisa *et al.* (Data set 1)[34] and The Cancer Genome Atlas (TCGA) (Data set 2)[35] was carried out. Relapse-free survival probability trended marginally higher ($P = 0.1$) for patients with tumour that had high *Dusp10* expression (Figure 7b, Data Set 1, left panel). After sample stratification for ERK2 expression, we found that high *Dusp10* in tumours was associated with approximately 20% improvement in survival probability of patients with high ERK2 expression (Figure 7b, Data Set 1, right panel). Such advantage was lost in this cohort of patients with low ERK2 expression in their tumours (Supplementary Figure S12). Similarly, we found that increased *Dusp10* expression resulted in better survival for CRC patients from TCGA (Figure 7b, Data Set 2). Interestingly, the benefit of *Dusp10* expression was not only observed after sample stratification for high ERK2 expression but also in all patients with high *Dusp10* level (without ERK2 stratification). Approximately 20% improvement in survival up to 60 months was observed in patients with high *Dusp10* from this data set. This shows that *Dusp10* upregulation increases patient survival independent of ERK2 level. Differences in the *Dusp10-ERK2* relation between the two data sets may reflect possible differences in patients' demographics, treatments and stage of tumour development at time of tissue sampling. At this point, we are not able to confirm whether the anti-tumour effect of DUSP10 is dependent on ERK2 expression. However, it is clear that increased *Dusp10* did resulted in better overall patients survival in both sets of data that were analysed.

To further understand the role of DUSP10 in CRC cell proliferation, we overexpressed DUSP10 in two human CRC cell lines, Caco2 and RCM-1. Proliferation was retarded in the cells overexpressing DUSP10 (Figure 7c). Interestingly, increased percentage of apoptotic cells (Annexin $V^+$+Annexin $V^+$7ADD$^-$) in DUSP10 overexpressing cells in response to the treatment of sulindac sulphide and cisplatin, two drugs that could induce apoptosis, was observed compared with control cells (Supplementary Figure S13). Furthermore, NOD/SCID mouse xenograft of Caco2 cells showed that overexpression of DUSP10 resulted in smaller tumours after the xenograft was allowed to develop for 3 weeks (Figure 7d). Together, these results indicated that higher DUSP10 expression in tumour cells could inhibit cell proliferation, which could be one of the factors leading to a better survival of patients compared to those having lower DUSP10 but high ERK2 expression in their tumours.

## DISCUSSION

DUSP10 was shown to be an inhibitor of inflammation.[36,37] In this study, we found that deficiency of DUSP10 in mice resulted in a better recovery from colonic damage with less inflammation (Figures 1a and d), suggesting that a protective mechanism limiting the amount of gut inflammation after colonic damage must be present in the KO mice. This could be provided by the IEC layer, which physically separates the underlying immune compartment from the luminal contents. Normally, administration of DSS will damage the mucus lining of the intestine. In turn, IEC will be exposed to DSS as well as to luminal antigens that have penetrated the damaged mucus layer. Activation of pro-inflammatory responses from the underlying immune compartment by the luminal contents will then occur after breaching of IEC barrier.[38] At this time, increase rate of epithelial wound healing function will allow the IEC layer to maintain the protective barrier. We observed better IEC barrier function in DUSP10 KO mice in response to DSS treatment than in WT mice (Figure 1e), in line with increased IEC proliferation in the KO colon (Figure 4). On the other hand, overexpression of DUDSP10 in IECs inhibited cell growth and wound healing (Figures 3e and f). Therefore, reduced inflammation in DUSP10 KO mice in response to DSS treatment is likely due to increased epithelial cell proliferation that resulted in increased IEC barrier function. However, when the threshold for IEC wound recovery is exceeded and can no longer control the damage, an increase in the underlying immune response will occur. This can lead to the expected excessive pro-inflammatory response, which further damage the epithelium. In fact, such phenotype was observed when 3% DSS was given instead of 2% DSS (Supplementary Figure S14). Of note, this study is different from a previous MKP1/IL10$^{-/-}$ colitis model,[17] which is an inherent spontaneous colitis model (due to the loss of IL10) that demonstrated a role of MKP1 (DUSP1 and not DUSP10) in Th1 and Th17 responses. Our work demonstrates the importance of DUSP10 in IEC function in relation to gut inflammation independent of other predefined gene mutation or immune deregulation.

In the intestine, two key processes of injury repair: epithelial cell proliferation and migration,[39] were increased in KO mice (Figure 4). These two processes go hand in hand to ensure that damaged and shed epithelial cells are replaced in time so that the epithelium maintains its continuity and barrier function. Such process is beneficial when is regulated as seen from our mouse colitis model, where gut inflammation was reduced in the KO mice. However, deregulation of IEC proliferation with excessive cell growth may lead to the development of intestinal cancer. Indeed, DUSP10 KO developed more tumours and of larger size after AOM/DSS administration (Figure 5). Gut inflammation that may contribute to the development of tumours was comparable between KO and WT colon particularly in normal region of the colon adjacent to the tumours, which provide indications of early events in tumour development. Only *Cxcl1* mRNA was increased in the tumours of KO mice that may be a response secondary to the increase in tumour development since the epithelial cells express *Cxcl1* promote tumour growth.[40] On the other hand, *Ptprc* mRNA, a pan-leukocytes marker, was decreased in KO tumour. This in all showed that inflammation is unlikely a key factor that leads to the difference in tumour development between WT and KO mice.

Having shown that DUSP10 is important for regulating tumorigensis in animal models, we attempted to identify evidence of the role of DUSP10 in human CRC. Previous genome-wide screens had identified gene polymorphisms within the regulatory region of Dusp10 and altered expression of *Dusp10* in CRC,[41–44] while others have reported increased expression of DUSP10 and other DUSPs in CRC.[45–47] Most of these studies speculated that DUSPs expression, particularly DUSP4/MKP2 and DUSP6/MKP3, may merely reflect excessive ERK1/2 activation in the tumours. Intriguingly, DUSP10 protein level was inversely correlated to the level of p-ERK1/2 in six human CRC cell lines (Figure 7a). Although, the number of cell lines examined was not exhaustive, it showed that increased DUSP10 is not just an indicator of increased ERK1/2 activity. Our results so far had supported the role of DUSP10 as potential colorectal tumour suppressor. Survival analysis (Figure 7b) based on the data from Marisa *et al.*[34] and TCGA[35] provided new insights about the involvement of DUSP10 in human CRC. There is overall increase in patients' relapse-free survival when *Dusp10* expression is upregulated. Furthermore, analysis of TCGA data showed that *Dusp10* mRNA was increased in the tumour compared with normal tissue adjacent to the tumours

(Supplementary Figure S15), which is in line with that found by Nomura *et al*.[45] This implies that increase in *Dusp10* expression occurs as the tumours develop. On the basis of the findings from our study, we propose that increase in *Dusp10* may be required for the control of tumour growth. In the absence of severe abnormalities, overexpression of *Dusp10* at the level found in the tumours is not needed. Particularly if the level of MAPKs activation is low (hence there is no need for feedback control) or when normal level of MAPKs activation is required (at state of homeostasis). Although the human CRC results may be preliminary, it showed a clear improvement in survival probability of patients who had high *DUSP10* expression among all tumours with high ERK2 expression. This implied that DUSP10 has a more complex role in CRC other than a feedback mechanism of increased ERK1/2. Nevertheless, due to the heterogeneity of CRC, further investigation of DUSP10 in various CRC subtypes needs to be done to fully understand the contribution of DUSP10 in CRC pathogenesis. Examination in different cohort of CRC patients and assessment of the effect of DUSP10 in a larger range of CRC cells with comprehensive genetic profiling will be valuable to understand the role of DUSP10 in cancer development. This will be particularly important for the identification of possible subgroup effect of DUSP10 as a tumour suppressor.

In summary, our data support an inhibitory role of DUSP10 in intestinal IEC barrier function *via* inhibition of ERK1/2 activation and KLF5 expression. This subsequently reduced IEC proliferation required for intestinal healing and barrier function after injury. Our work demonstrates the importance of DUSP10 in IEC function in relation to gut inflammation, and shows that DUSP10 has a role in CRC development. The loss of DUSP10 resulted in increased epithelial cell proliferation and wound healing, which are key protective factors to reduce intestinal inflammation. However, deleterious effect will occur when such proliferation is not kept in check or when the intestine is subjected to insults (such as carcinogen) leading to the development of cancer-associated mutation. As seen in the DUSP10 mice, when subjected to AOM carcinogen and chronic DSS treatment, the increase in epithelial cell proliferation potential became a key cause for more tumours in the colon.

Currently, cetuximab is an anti-EGFR mAb that is used clinically for CRC treatment. This therapy targets the upstream EGFR in the hope of providing a broad effect to limit ERK1/2 activity. However, success of this monotherapy is limited, particularly in CRC with KRAS-BRAF mutation where ERK activation was not sufficiently downregulated by anti-EGFR mAb treatment.[48] This suggested that a more ERK directed therapy might be useful in these patients, together with other CRC pathway targeting drugs (that is, targeting PI3K/AKT). Our study showed that DUSP10 inhibits IEC proliferation via ERK, which suggests an inherent host response to limit colorectal tumour growth. Both our DUSP10 KO mice model and analysis of human CRC survival data are concordant for DUSP10 as a potential colorectal tumour suppressor. Hence, the regulation of DUSP10 may be targeted as part of CRC therapy in a well-defined patient cohort with low *Dusp10* expression and high ERK1/2 activity. DUSPs, including DUSP10, are active once expressed. However, their activities could be regulated at multiple levels.[49] It has been shown that the transcription of several DUSPs, including DUSP10, could be induced by extracellular stimuli.[36,50] For instance, the expression of DUSP10 in macrophages can be induced by lipopolysaccharide. This could potentially reflect a natural feedback mechanism for the suppression of MAPKs activity that regulates the inflammatory response, which can be quickly terminated once it is not required to prevent deleterious excessive inflammation. On the other hand, posttranslational modification such as acetylation and phosphorylation regulates their stability and/or activity. For example, acetylation of DUSP1 has been shown to increase its activity.[51] Inhibition of deacetylases increases DUSP1 acetylation thereby increases its activity, which resulted in reduced inflammation and mortality in mice treated with lipopolysaccharide. In addition, phosphorylation and dephosphorylation of DUSPs could change their half-life and/or activities. Understanding the mechanisms regulating the expression and activity of DUSP10 will be beneficial for targeting this protein for CRC treatment. Moreover, continue efforts to investigate IEC interactions with gut immune cells in our mouse model will also provide valuable insights to the complex role of DUSPs/MKPs in intestinal inflammation and gut IEC functions.

## MATERIALS AND METHODS

### Animal studies

Animal studies were approved by the National University of Singapore Institutional Animal Care and Use Committee. The MKP5-deficient mice generated previously[36] were crossed with C57BL/6 mice for 12 generations. WT and KO pups from the same heterozygous breeders ($MKP5^{+/-} \times MKP5^{+/-}$) were used to establish the MKP5 WT and KO colonies and the two colonies were maintained separately. NOD/SCID mice were purchased from Invivos Pte Ltd, Singapore. For induction of acute colitis, 8-week-old male mice were given 2% DSS (molecular weight, 35 000–50 000; MP Biomedicals Solon, OH, USA) in sterile drinking water for 5 days. During recovery, mice were given sterile drinking water. Colon specimens were prepared as Swiss rolls for fixation in 10% neutral buffered formalin before embedding in paraffin for section and standard haematoxylin and eosin (H&E) staining. Blinded histological assessments were conducted as described (Supplementary Table 1).[52] Details for immunohistochemical staining of tissues were summarised in Supplementary Methods.

For induction of colon tumours, 10-week-old mice (9–12 mice per group) were given a single intra-peritoneal injection of 10 mg/kg AOM (Sigma-Aldrich, St Louis, MO, USA) and allowed to rest for 1 week before initiation of 3 cycles of 1% DSS administration for 5 days with 2 weeks rest. Mice were killed on Week 15 for the assessment of tumour incidence, multiplicity and size under an observation microscope. Histological assessment of intestinal neoplasm was as described previously[53] and the size of each tumour was measured along the widest length of the tumour mass. Tumour inflammation was scored based on criteria described in Supplementary Table 2.

CRC xenograft was established by injection of $5 \times 10^6$ Caco2 cells subcutaneously into the flanks of 6-week-old female NOD/SCID mice. Tumours were allowed to develop for 3 weeks before harvest for analysis. The relative size of tumours was calculated using the formula; $(L \times W)/2$, where $L$ and $W$ are longest and shortest diameter of the tumour, respectively.

### Assessment of intestinal permeability, colonic IEC migration/proliferation

Mice were orally gavaged with 0.5 mg/g body weight of FITC-dextran (molecular weight, 3000–5000; Sigma-Aldrich). Serum FITC-dextran concentrations were assessed after 4 h by measuring fluorescence at 520 nm (excitation at 490 nm) using Biotek Synergy H1 Hybrid Multi-Mode Microplate Reader versus a FITC-dextran standard curve and normalised to total serum protein. To assess IEC migration, mice were injected intraperitoneally with 100 μg/g body weight of 5-bromo-2-deoxyuridine (BrdU; Sigma, St Louis, MO, USA) 24 h before killing. Cells incorporated with BrdU were stained using the BrdU staining kit (Invitrogen, Carlsbad, CA, USA). Proliferating cells were determined by immunohistochemical staining using anti-Ki67 antibody (eBioscience, San Diego, CA, USA) (see Supplementary Methods).

### *In vitro* wound healing

Post-confluent CMT93 cells stably overexpressing *Dusp10/Mkp5* or control pCDNA (vector) were treated with 5% DSS for 24 h (except for untreated group) before wounding using scratch assay. Each wound was photographed and measured at six pre-marked positions at Time 0 and Time 7 h post wounding. Wound size was measured using Adobe Photoshop software (Adobe, San Jose, CA, USA). Wound recovery is expressed as percentage wound closure after 7 h post scratch.

### Cell proliferation assay

In all, $0.2 \times 10^6$ CMT93 cells were seeded and serum starved for 24 h (Day 0) before DMEM containing 10% FBS was added for cells to grow for another 24 h in standard culture medium with or without 5% DSS (Day 1). Total cell proliferation is expressed as percentage relative to the number of cells at Day 0. Cell number was determined using crystal violet staining (see Supplementary Methods). Experiment was repeated three times with six replicates/time point.

### Hang-drop cancer cell spheroid culture

Hang-drop culture was performed as described (see Supplementary Methods).[54] Spheroids were harvested on Day 5 and measured according to '($a$+$b$)/2', where $a$ = long half axis and $b$ = short half axis of the spheroid.[55] This was further normalised to the initial seeding density to account for possible slight differences in initial cell count and expressed as relative spheroid size.

### Nucleic acid isolation and analysis

Total RNA was extracted in TRIzol (Invitrogen) based on the manufacturer's instructions. RNA extracted from specimen exposed to DSS was purified to isolate DSS-free mRNA using Dynabeads mRNA DIRECT Kit (Invitrogen). Complementary DNA (cDNA) was synthesised using GoScript Reverse Transcription System (Promega, Madison, WI, USA). Real-time qPCR was performed using Bio-rad CFX Connect real-time PCR system and reagents (Bio-Rad Laboratories, Hercules, CA, USA). Relative fold change of target genes was calculated using the Pfaffl method.[56] Primers used for qPCR are detailed in Supplementary Table 3.

### Western blot

Cells and tissues were homogneised in lysis buffer (1M Tris-Cl, 5M NaCl, 10% NP-40) containing Halt Protease and Phosphatase Inhibitor Cocktail and 5 mM EDTA (Thermo Scientific, Waltham, MA, USA). Total proteins were resolved in Tris/Glycine gel (10 or 12% acrylamide, 1.5M Tris (pH 8.8), 10% SDS, 10% APS, TEMED) before transferred onto PVDF membrane for detection of proteins (see Supplementary Methods). The antibodies used are summarised in Supplementary Table 4. ImageJ software was used for densitometry analysis.[57]

### Colorectal patient survival data analysis

For survival data analysis of colorectal tumours, we applied two data sets: (1) microarray gene expression data downloaded from GEO database with accession number GSE39582[34] and (2) Level-3 RNA-seq data from TCGA data portal (colon adenocarcinoma).[35] Normalisation of gene expression was performed across all samples based on the cross correlation method,[58] while normalisation of RNA-seq data was carried out using the total numbers of mappable reads across all samples. When using normalised ERK2/DUSP10 expression data to classify ERK2/DUSP10 high and low samples, we first used the ERK2/DUSP10 median expression to separate high and low expression samples. Then, we removed those middle samples with expression levels 87% higher but 115% lower than the median expression value to minimize the false discovery in classification. The survival analysis was based on the Kaplan–Meier method for two group samples of low and high *DUSP10* expression.

### Statistics

All statistical analyses were performed using Graphpad Prism v4.03 software (GraphPad, La Jolla, CA, USA). Non-parametric, Mann–Whitney test was used in all comparisons unless otherwise stated.

Additional information is available in Supplementary Methods.

## CONFLICT OF INTEREST

The authors declare no conflict of interest.

## ACKNOWLEDGEMENTS

We would like to thank Nicholas Gascoigne for advice and helpful discussion. This study was supported by grants from the Office of Deputy President, National University of Singapore, the Ministry of Education (MOE2010-T2-1-079) and the National Medical Research Council (IRG10nov091 and CBRG11nov101) of Singapore.

## REFERENCES

1 Podolsky DK. Inflammatory bowel disease. *N Engl J Med* 2002; **347**: 417–429.
2 Rimoldi M, Chieppa M, Salucci V, Avogadri F, Sonzogni A, Sampietro GM *et al.* Intestinal immune homeostasis is regulated by the crosstalk between epithelial cells and dendritic cells. *Nat Immunol* 2005; **6**: 507–514.
3 Radtke F, Clevers H. Self-renewal and cancer of the gut: two sides of a coin. *Science* 2005; **307**: 1904–1909.
4 Koch S, Nava P, Addis C, Kim W, Denning TL, Li L *et al.* The Wnt antagonist Dkk1 regulates intestinal epithelial homeostasis and wound repair. *Gastroenterology* 2011; **141**: 68 e1–68 e8.
5 Egan LJ, de Lecea A, Lehrman ED, Myhre GM, Eckmann L, Kagnoff MF *et al.* Nuclear factor-kappa B activation promotes restitution of wounded intestinal epithelial monolayers. *Am J Physiol Cell Physiol* 2003; **285**: C1028–C1035.
6 Matsubayashi Y, Ebisuya M, Honjoh S, Nishida E. ERK activation propagates in epithelial cell sheets and regulates their migration during wound healing. *Curr Biol* 2004; **14**: 731–735.
7 Zhang J, Owen CR, Sanders MA, Turner JR, Basson MD. The motogenic effects of cyclic mechanical strain on intestinal epithelial monolayer wound closure are matrix dependent. *Gastroenterology* 2006; **131**: 1179–1189.
8 Pai R, Ohta M, Itani RM, Sarfeh IJ, Tarnawski AS. Induction of mitogen-activated protein kinase signal transduction pathway during gastric ulcer healing in rats. *Gastroenterology* 1998; **114**: 706–713.
9 Lee SH, Hu LL, Gonzalez-Navajas J, Seo GS, Shen C, Brick J *et al.* ERK activation drives intestinal tumorigenesis in Apc(min/+) mice. *Nat Med* 2010; **16**: 665–670.
10 Oliveira C, Velho S, Moutinho C, Ferreira A, Preto A, Domingo E *et al.* KRAS and BRAF oncogenic mutations in MSS colorectal carcinoma progression. *Oncogene* 2007; **26**: 158–163.
11 Fearon ER. Molecular genetics of colorectal cancer. *Annu Rev Pathol* 2011; **6**: 479–507.
12 Delaunoit T, Limburg PJ, Goldberg RM, Lymp JF, Loftus EV Jr.. Colorectal cancer prognosis among patients with inflammatory bowel disease. *Clin Gastroenterol Hepatol* 2006; **4**: 335–342.
13 Hrabe JE, Byrn JC, Button AM, Zamba GK, Kapadia MR, Mezhir JJ *et al.* A matched case-control study of IBD-associated colorectal cancer: IBD portends worse outcome. *J Surg Oncol* 2013; **109**: 117–121.
14 Farooq A, Zhou MM. Structure and regulation of MAPK phosphatases. *Cell Signal* 2004; **16**: 769–779.
15 Cornell TT, Fleszar A, McHugh W, Blatt NB, Le Vine AM, Shanley TP *et al.* Mitogen-activated protein kinase phosphatase 2, MKP-2, regulates early inflammation in acute lung injury. *Am J Physiol Lung Cell Mol Physiol* 2012; **303**: L251–L258.
16 Shi H, Verma M, Zhang L, Dong C, Flavell RA, Bennett AM *et al.* Improved regenerative myogenesis and muscular dystrophy in mice lacking Mkp5. *J Clin Invest* 2013; 2064–2077.
17 Matta R, Barnard JA, Wancket LM, Yan J, Xue J, Grieves J *et al.* Knockout of Mkp-1 exacerbates colitis in Il-10-deficient mice. *Am J Physiol Gastrointest Liver Physiol* 2012; **302**: G1322–G1335.
18 Nandan MO, McConnell BB, Ghaleb AM, Bialkowska AB, Sheng H, Shao J *et al.* Krüppel-like factor 5 mediates cellular transformation during oncogenic KRAS-induced intestinal tumorigenesis. *Gastroenterology* 2008; **134**: 120–130.
19 Nandan MO, Chanchevalap S, Dalton WB, Yang VW. Krüppel-like factor 5 promotes mitosis by activating the cyclin B1/Cdc2 complex during oncogenic Ras-mediated transformation. *FEBS Lett* 2005; **579**: 4757–4762.
20 Conkright MD, Wani MA, Anderson KP, Lingrel JB. A gene encoding an intestinal-enriched member of the Krüppel-like factor family expressed in intestinal epithelial cells. *Nucleic Acids Res* 1999; **27**: 1263–1270.
21 McConnell BB, Kim SS, Bialkowska AB, Yu K, Sitaraman SV, Yang VW *et al.* Krüppel-like factor 5 protects against dextran sulfate sodium-induced colonic injury in mice by promoting epithelial repair. *Gastroenterology* 2011; **140**: 540–549.e2.
22 McConnell BB, Kim SS, Yu K, Ghaleb AM, Takeda N, Manabe I *et al.* Krüppel-like factor 5 is important for maintenance of crypt architecture and barrier function in mouse intestine. *Gastroenterology* 2011; **141**: 1302–1313. 1313.e1-6.
23 Yang Y, Goldstein BG, Nakagawa H, Katz JP. Krüppel-like factor 5 activates MEK/ERK signaling via EGFR in primary squamous epithelial cells. *FASEB J* 2007; **21**: 543–550.
24 Mori A, Moser C, Lang SA, Hackl C, Gottfried E, Kreutz M *et al.* Up-regulation of Krüppel-like factor 5 in pancreatic cancer is promoted by interleukin-1beta signaling and hypoxia-inducible factor-1alpha. *Mol Cancer Res* 2009; **7**: 1390–1398.
25 Usui S, Sugimoto N, Takuwa N, Sakagami S, Takata S, Kaneko S *et al.* Blood lipid mediator sphingosine 1-phosphate potently stimulates platelet-derived growth factor-A and -B chain expression through S1P1-Gi-Ras-MAPK-dependent induction of Kruppel-like factor 5. *J Biol Chem* 2004; **279**: 12300–12311.

26 Tanoue T, Moriguchi T, Nishida E. Molecular cloning and characterization of a novel dual specificity phosphatase, MKP-5. *J Biol Chem* 1999; **274**: 19949–19956.
27 Theodosiou A, Smith A, Gillieron C, Arkinstall S, Ashworth A. MKP5, a new member of the MAP kinase phosphatase family, which selectively dephosphorylates stress-activated kinases. *Oncogene* 1999; **18**: 6981–6988.
28 Sun R, Chen X, Yang VW. Intestinal-enriched Krüppel-like factor (Krüppel-like factor 5) is a positive regulator of cellular proliferation. *J Biol Chem* 2001; **276**: 6897–6900.
29 McConnell BB, Bialkowska AB, Nandan MO, Ghaleb AM, Gordon FJ, Yang VW *et al.* Haploinsufficiency of Krüppel-like factor 5 rescues the tumor-initiating effect of the Apc(Min) mutation in the intestine. *Cancer Res* 2009; **69**: 4125–4133.
30 De Robertis M, Massi E, Poeta ML, Carotti S, Morini S, Cecchetelli L *et al.* The AOM/DSS murine model for the study of colon carcinogenesis: From pathways to diagnosis and therapy studies. *J Carcinog* 2011; **10**: 9.
31 Bienz M, Clevers H. Linking colorectal cancer to Wnt signaling. *Cell* 2000; **103**: 311–320.
32 Takahashi M, Nakatsugi S, Sugimura T, Wakabayashi K. Frequent mutations of the beta-catenin gene in mouse colon tumors induced by azoxymethane. *Carcinogenesis* 2000; **21**: 1117–1120.
33 Takahashi M, Wakabayashi K. Gene mutations and altered gene expression in azoxymethane-induced colon carcinogenesis in rodents. *Cancer Sci* 2004; **95**: 475–480.
34 Marisa L, de Reyniès A, Duval A, Selves J, Gaub MP, Vescovo L *et al.* Gene expression classification of colon cancer into molecular subtypes: characterization, validation, and prognostic value. *PLoS Med* 2013; **10**: e1001453.
35 Cancer Genome Atlas Network Comprehensive molecular characterization of human colon and rectal cancer. *Nature* 2012; **487**: 330–337.
36 Zhang Y, Blattman JN, Kennedy NJ, Duong J, Nguyen T, Wang Y *et al.* Regulation of innate and adaptive immune responses by MAP kinase phosphatase 5. *Nature* 2004; **430**: 793–797.
37 Qian F, Deng J, Gantner BN, Flavell RA, Dong C, Christman JW *et al.* Map kinase phosphatase 5 protects against sepsis-induced acute lung injury. *Am J Physiol Lung Cell Mol Physiol* 2012; **302**: L866–L874.
38 Kinnebrew MA, Pamer EG. Innate immune signaling in defense against intestinal microbes. *Immunol Rev* 2012; **245**: 113–131.
39 Sturm A, Dignass AU. Epithelial restitution and wound healing in inflammatory bowel disease. *World J Gastroenterol* 2008; **14**: 348–353.
40 Wang D, Wang H, Brown J, Daikoku T, Ning W, Shi Q *et al.* CXCL1 induced by prostaglandin E2 promotes angiogenesis in colorectal cancer. *J Exp Med* 2006; **203**: 941–951.
41 Zhang T, Li X, Du Q, Gong S, Wu M, Mao Z *et al.* DUSP10 gene polymorphism and risk of colorectal cancer in the Han Chinese population. *Eur J Cancer Prev* 2014; **23**: 173–176.
42 Houlston RS, Cheadle J, Dobbins SE, Tenesa A, Jones AM, Howarth K *et al.* Meta-analysis of three genome-wide association studies identifies susceptibility loci for colorectal cancer at 1q41, 3q26.2, 12q13.13 and 20q13.33. *Nat Genet* 2010; **42**: 973–977.
43 Spain SL, Carvajal-Carmona LG, Howarth KM, Jones AM, Su Z, Cazier JB *et al.* Refinement of the associations between risk of colorectal cancer and polymorphisms on chromosomes 1q41 and 12q13.13. *Hum Mol Genet* 2012; **21**: 934–946.
44 Whiffin N, Dobbins SE, Hosking FJ, Palles C, Tenesa A, Wang Y *et al.* Deciphering the genetic architecture of low-penetrance susceptibility to colorectal cancer. *Hum Mol Genet* 2013; **22**: 5075–5082.
45 Nomura M, Shiiba K, Katagiri C, Kasugai I, Masuda K, Sato I *et al.* Novel function of MKP-5/DUSP10, a phosphatase of stress-activated kinases, on ERK-dependent gene expression, and upregulation of its gene expression in colon carcinomas. *Oncol Rep* 2012; **28**: 931–936.
46 Popovici V, Budinska E, Tejpar S, Weinrich S, Estrella H, Hodgson G *et al.* Identification of a poor-prognosis BRAF-mutant-like population of patients with colon cancer. *J Clin Oncol* 2012; **30**: 1288–1295.
47 Gröschl B, Bettstetter M, Giedl C, Woenckhaus M, Edmonston T, Hofstädter F *et al.* Expression of the MAP kinase phosphatase DUSP4 is associated with microsatellite instability in colorectal cancer (CRC) and causes increased cell proliferation. *Int J Cancer* 2013; **132**: 1537–1546.
48 Misale S, Yaeger R, Hobor S, Scala E, Janakiraman M, Liska D *et al.* Emergence of KRAS mutations and acquired resistance to anti-EGFR therapy in colorectal cancer. *Nature* 2012; **486**: 532–536.
49 Liu Y, Shepherd EG, Nelin LD. MAPK phosphatases--regulating the immune response. *Nat Rev Immunol* 2007; **7**: 202–212.
50 Zhao Q, Wang X, Nelin LD, Yao Y, Matta R, Manson ME *et al.* MAP kinase phosphatase 1 controls innate immune responses and suppresses endotoxic shock. *J Exp Med* 2006; **203**: 131–140.
51 Cao W, Bao C, Padalko E, Lowenstein CJ. Acetylation of mitogen-activated protein kinase phosphatase-1 inhibits Toll-like receptor signaling. *J Exp Med* 2008; **205**: 1491–1503.
52 Heazlewood CK, Cook MC, Eri R, Price GR, Tauro SB, Taupin D *et al.* Aberrant mucin assembly in mice causes endoplasmic reticulum stress and spontaneous inflammation resembling ulcerative colitis. *PLoS Med* 2008; **5**: e54.
53 Turusov VS, Mohr U. International Agency for Research on Cancer, International Life Sciences Institute *Pathology of Tumours in Laboratory Animals*. 2nd edn International Agency for Research on Cancer: Lyon, 1990.
54 Foty R. A simple hanging drop cell culture protocol for generation of 3D spheroids. *J Vis Exp* 2011; **51**: 2720–2723.
55 Zhang X, Wang W, Yu W, Xie Y, Zhang Y, Ma X *et al.* Development of an in vitro multicellular tumor spheroid model using microencapsulation and its application in anticancer drug screening and testing. *Biotechnol Prog* 2005; **21**: 1289–1296.
56 Pfaffl MW. A new mathematical model for relative quantification in real-time RT-PCR. *Nucleic Acids Res* 2001; **29**: e45.
57 Schneider CA, Rasband WS, Eliceiri KW. NIH Image to ImageJ: 25 years of image analysis. *Nat Methods* 2012; **9**: 671–675.
58 Chua SW, Vijayakumar P, Nissom PM, Yam CY, Wong VV, Yang H *et al.* A novel normalization method for effective removal of systematic variation in microarray data. *Nucleic Acids Res* 2006; **34**: e38.

Supplementary Information accompanies this paper on the Oncogene website (http://www.nature.com/onc)